Physics and Imaging in Radiation Oncology 33 (2025) 100727

Contents lists available at ScienceDirect

Physics and Imaging in Radiation Oncology

journal homepage: www.sciencedirect.com/journal/physics-and-imaging-in-radiation-oncology

Original Research Article

Optimizing the dose-averaged linear energy transfer for the dominant intraprostatic lesions in high-risk localized prostate cancer patients

Bo Zhao [a,*], Nobuyuki Kanematsu [a,*], Shuri Aoki [b], Shinichiro Mori [a], Hideyuki Mizuno [a], Takamitsu Masuda [a], Hideyuki Takei [a], Hitoshi Ishikawa [b]

[a] Department of Accelerator and Medical Physics, Institute for Quantum Medical Science, National Institutes for Quantum Science and Technology (QST), Chiba, Japan
[b] QST Hospital, National Institutes for Quantum Science and Technology, Chiba, Japan

ARTICLE INFO

Keywords:
Localized prostate cancer
Carbon-ion radiotherapy
LET painting
Dose-averaged LET
Focal boost

ABSTRACT

Background and purpose: Radiotherapy for localized prostate cancer often targets the entire prostate with a uniform dose despite the presence of high-risk dominant intraprostatic lesions (DILs). This study investigated the feasibility of focal dose-averaged linear energy transfer (LET_d) boost for prostate carbon-ion radiotherapy to deposit higher LET_d to DILs while ensuring desired relative biological effectiveness weighted dose coverage to targets and sparing organs at risk (OARs).

Materials and methods: A retrospective planning study was conducted on 15 localized prostate cancer cases. The DILs were identified on multiparametric MRI and used to define the boost target (PTV_{boost}). Two treatment plans were designed for each patient: 1) conventional plan optimized by the single-field uniform dose technique, and 2) boost plan optimized by the multifield optimization and LET painting technique, to achieve LET_d boost within the PTV_{boost}. Dose and LET_d metrics of the targets and OARs were compared between the two plans.

Results: Compared to the conventional plans, the boost plans delivered clinically acceptable dose coverage ($D_{90\%}$ and $D_{50\%}$) to the target (PTV2) within 1% differences while significantly increasing the minimum LET_d by 16 ~ 24 keV/μm for the PTV_{boost} (63.9 ± 2.8 vs. 44.0 ± 1.3 keV/μm, $p < 0.001$). Furthermore, these improvements were consistent across all cases, irrespective of their anatomical features, including the boost volume's size, location, and shape.

Conclusion: Focal LET_d boost was a feasible strategy for prostate carbon-ion radiotherapy. This investigation demonstrated its superiority in delivering LET_d boost without depending on tumor location and volume across different cases.

1. Introduction

Radiotherapy for localized prostate cancer commonly targets the whole prostate volume with a uniform prescribed dose based on the assumption of multifocality in prostate cancer [1]. Nonetheless, it is known that prostate cancers typically suffer from severe hypoxia [2], and histopathological investigations revealed the presence of dominant intraprostatic lesions (DILs) in the prostate gland [3]. The DILs denote the specific area that contains the most high-grade, aggressive cancer foci [4]. Often, these DILs comprise a small portion of the prostate's total volume, yet they frequently serve as the primary sites of recurrence following radiotherapy [5]. Gomez-Iturriaga et al. showed that selectively boosting the dose to the DILs while irradiating the entire prostate can improve the tumor control probability (TCP) [6]. Therefore, dose escalation specifically targeting DILs, or focal boosting in prostate cancer radiotherapy, is of significant clinical interest.

Clinical trials and planning studies of various treatment strategies for dose escalation within prostate DILs have been reported, encompassing both photon external beam radiotherapy (EBRT) and intensity-modulated proton therapy (IMPT) [7]. The FLAME study was the largest clinical trial undertaken thus far, and it showed a noteworthy improvement in the 5-year biochemical disease-free survival (bDFS) for patients in the focal boost treatment arm [8,9]. Other clinical studies, including ASCENDE-RT and HYPRO, reported improved tumor control with focal boost radiotherapy [10,11]. However, these studies showed that dose-escalation to the DILs might increase the risk of toxicity to

* Corresponding authors at: Department of Accelerator and Medical Physics, Institute for Quantum Medical Science, National Institutes for Quantum Science and Technology (QST), 4-9-1 Anagawa, Inage-ku, Chiba 263-8555, Japan.
E-mail addresses: zhao.bo@qst.go.jp (B. Zhao), kanematsu.nobuyuki@qst.go.jp (N. Kanematsu).

https://doi.org/10.1016/j.phro.2025.100727
Received 18 July 2024; Received in revised form 4 February 2025; Accepted 5 February 2025
Available online 7 February 2025

Table 1
Target goals and OAR constraints for both conventional and boost plans. It should be noted that all the dose metrics are defined as RBE-weighted values. Abbreviations: OAR: organs at risk; PTV: planning target volume; LET_d: dose-averaged linear energy transfer; PRV: planning risk volume.

Types	Targets or OARs	Goals or constraints
Targets goals	PTV1	$D_{min} \geq 32.68$ Gy
	PTV2	$D_{min} \geq 49.02$ Gy, $D_{max} \leq 54.18$ Gy
	PTV_{boost}	to achieve LET_d as high as possible when variations in PTV2's $D_{90\%}$ and $D_{50\%}$ should be kept within 1% before and after LET optimization [22]
OAR constraints	Rectum	$D_{0.1\ cc} \leq 53$ Gy, $V_{50\ Gy} \leq 7\%$, $V_{40\ Gy} \leq 16\%$
	Urethra	$D_{0.1\ cc} \leq 51.6$ Gy
	PRV	

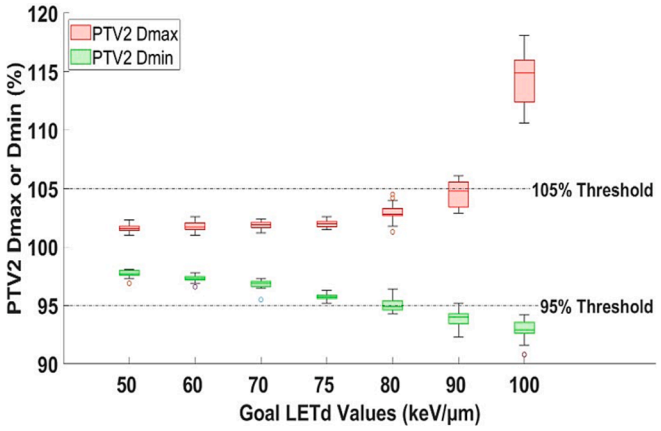

Fig. 1. A grouped boxplot graph of the PTV2 D_{max} (red boxes) and D_{min} (green boxes) of the boost plans for seven groups for all cases. Each group represented the goal LET_d values of 50, 60, 70, 75, 80, 90, and 100 keV/μm, respectively. The boxes showed the upper and lower quartiles and the horizontal lines in the boxes are medians. The whiskers showed 5–95 percentiles. Outliers were denoted with a circle. The upper horizontal dashed line indicated the threshold of PTV2 D_{max} at 105% of the prescribed dose, while the lower dashed line indicated the threshold of PTV2 D_{min} at 95%. (For interpretation of the references to colour in this figure legend, the reader is referred to the web version of this article.)

nearby or overlapped organs at risk (OARs), such as the rectum, urethra, and bladder. An EBRT study revealed that the boost volume overlapped with the surrounding OARs in 83% of patients [12]. Another stereotactic ablative radiation therapy investigation identified that the key determinant in achieving the desired dose of the boosting DILs was its margin overlapping with the rectum [13]. Similarly, a brachytherapy study found it challenging to satisfy the urethral dose constraints when the boost planning volumes are near the urethral structure [14]. Moreover, a proton therapy planning study demonstrated that focal boost plans resulted in a 2.3% higher normal tissue complication probability (NTCP) for the urethra than conventional plans, with a statistically significant difference [15]. FLAME trial's authors emphasized the need for further optimization of focal boost treatments to avoid increasing toxicity in the urethra and other OARs, highlighting this as a critical focus for future investigation [9].

Carbon ion radiotherapy (CIRT) offers a potentially effective approach for focal boost treatments [16]. Beyond delivering prescribed doses to targets, the linear energy transfer (LET) painting technique aims to concentrate high dose-averaged LET (LET_d) into sites with a high risk of recurrence, such as the intraprostatic DILs [5]. Relative biological effectiveness (RBE) is known to increase with LET, reaching its maximum at an LET of approximately 150 keV/μm, while oxygen enhancement ratio (OER) shows a declining trend as LET increases [17]. Tumors often exhibit significant hypoxia [18], and high LET irradiation is particularly effective in overcoming radioresistance in these hypoxic tumors [19]. Therefore, delivering higher LET radiation while maintaining the same RBE-weighted dose was assumed to improve TCP [20,21]. An initial clinical trial conducted by Koto et al. recently confirmed that LET painting was safe and effective for head and neck cancer CIRT [22]. Given these physical and radiobiological insights, employing the CIRT with the LET painting technique should facilitate focal LET_d boosting while minimizing the toxicities to adjacent OARs.

Notably, the clinical goals of carbon-ion LET painting-based boost differ from photon dose-escalation boost, which aims to improve local control. Since CIRT has already demonstrated outstanding tumor control for prostate cancer, radiation oncologists need to pay more attention to minimizing gastrointestinal (GI) and genitourinary (GU) side effects, while still ensuring effective tumor control [9,16]. Consequently, carbon-ion focal LET_d boost is beneficial for designing safer and lower-burden treatment strategies, including dose de-escalation in low-risk areas and ultra-hypofractionation (4 fractions or less) [23]. This retrospective treatment planning study aims to demonstrate the feasibility of the LET_d boosting approach and to develop benchmarks for future clinical practice.

The aim of this study was to analyze and compare the RBE-weighted dose and LET_d distributions, as well as the corresponding dose and LET_d metrics, between two treatment planning approaches. Specifically, we evaluated the conventional plan using the single-field uniform dose technique and the focal LET_d boost plan, hereinafter referred to as the "boost plan," optimized via multifield optimization and LET painting technique.

2. Materials and methods

2.1. Patient cases and contouring

This study analyzed 15 high-risk localized prostate cancer cases treated with CIRT between January 2021 and December 2022. Prostate volumes varied from 12.5 to 33.8 cm^3. DILs were contoured by experienced radiation oncologists, based on the multiparametric MRI (mp-MRI), which included T2-weighted (T2W), diffusion-weighted imaging (DWI), and dynamic contrast-enhanced (DCE) sequences [8,24]. The DIL was defined as GTV_{boost}, with an average volume of 0.6 ± 0.5 cm^3 (range 0.1–1.7 cm^3). For each case, the urethra was delineated on MRI scans. Then, the contours of both DIL and urethra were propagated from the MRI images to the planning CT scans using a multi-modality deformable registration tool based on a feature similarity scoring metric (MIM Software, Ohio, USA). This study has been approved by our institute's ethics committee and institutional review board (approval number: N23-009).

2.2. Treatment planning and optimization

Treatment plans were designed with an in-house treatment planning system (TPS), developed for pencil beam scanning carbon-ion radiation therapy [25]. The TPS can simultaneously optimize the RBE-weighted dose and LET_d distributions by setting a series of structures, priorities, objectives, goals, and weights. However, it currently lacks a robust optimization tool. The RBE was estimated with the modified microdosimetric kinetic model (modified MKM), as previously reported by Inaniwa et al. [26]. The LET_d at location $\boldsymbol{r}$, $LET_d(\boldsymbol{r})$, was calculated as follows [27]:

$$LET_d(\boldsymbol{r}) = \frac{\sum_j l_j(\boldsymbol{r}) \bullet d_j(\boldsymbol{r}) \bullet w_j}{\sum_j d_j(\boldsymbol{r}) \bullet w_j}$$

where $l_j(\boldsymbol{r})$ is the dose-averaged LET of the j th beamlet. w_j is the dose weight for j th beamlets. $d_j(\boldsymbol{r})$ is the physical dose deposited by the j th

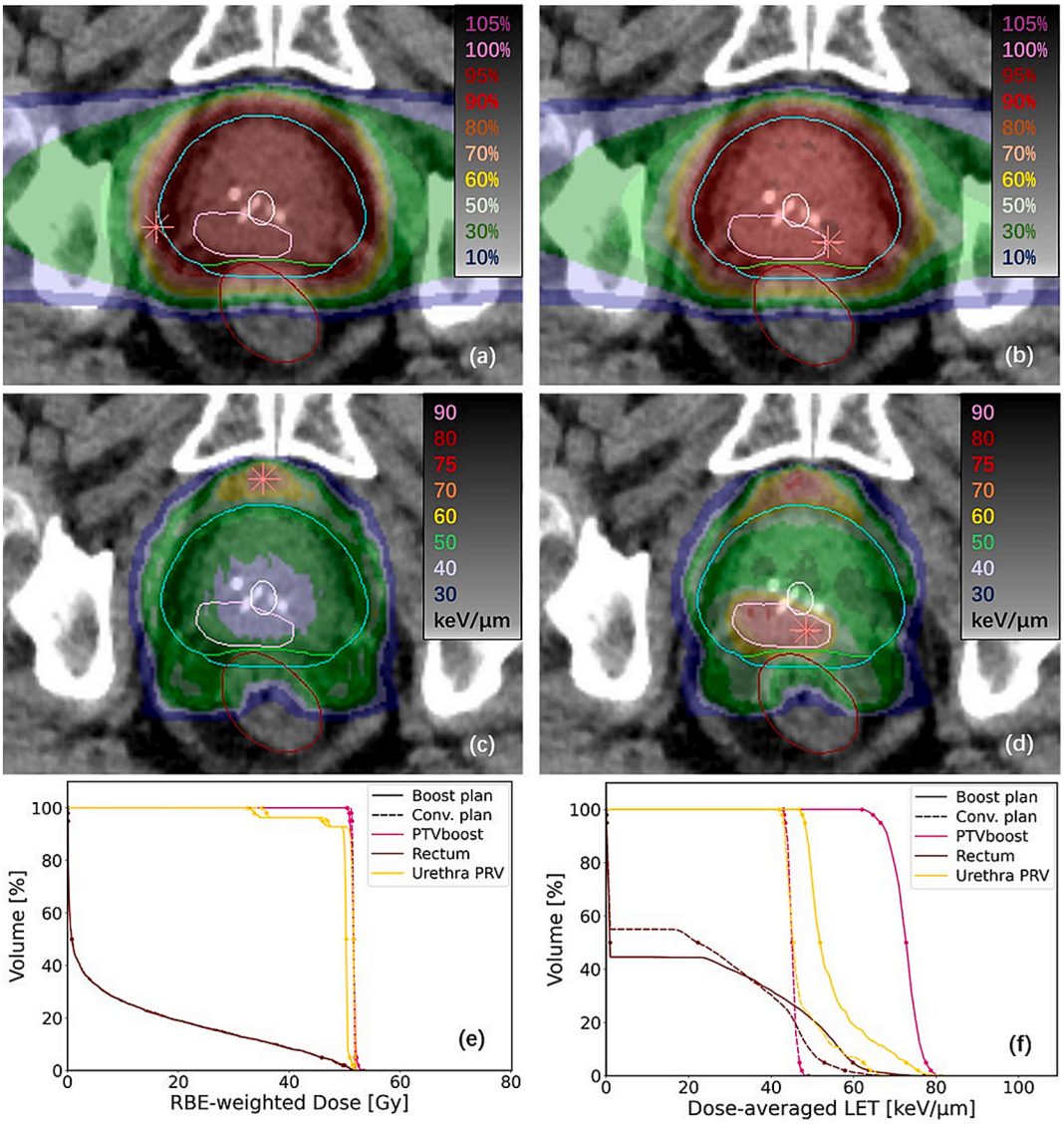

Fig. 2. Comparison of treatment plans for a typical case of localized prostate cancer, with the boost region before and after dose-averaged LET optimization. The cyan line represented PTV1, the green line PTV2, the pink line PTV_{boost}, the dark red line the rectum, and the yellow line the urethra PRV. The RBE-weighted dose distributions were shown for (a) the conventional plan and (b) the boost plan, while the dose-averaged LET distributions were shown for (c) the conventional plan and (d) the boost plan. Histogram comparisons between the two plans were presented in (e) DVHs and (f) LVHs, respectively. The line colors of PTV_{boost}, the rectum, and the urethra PRV were identical to their contour lines. The solid lines in the histograms represented the boost plan, and the dashed lines represented the conventional plan. (For interpretation of the references to colour in this figure legend, the reader is referred to the web version of this article.)

Table 2
Comparisons of the OAR constraints between conventional and boost plans for 15 cases. It should be noted that all the dose metrics are defined as RBE-weighted values. Abbreviations: OAR: organs at risk; Conv.: conventional; PRV: planning risk volume.

Constraints	Conv. Plan	Boost Plan	Mean Difference	p-val
Rectum $D_{0.1\ cc}$ (Gy)	50.33 ± 2.35	49.87 ± 3.40	−0.47 ± 1.12	0.68
Rectum $V_{50\ Gy}$ (%)	1.7 ± 2.0	1.7 ± 2.0	0.0 ± 0.2	0.99
Rectum $V_{40\ Gy}$ (%)	5.1 ± 4.1	4.7 ± 4.1	−0.5 ± 0.3	0.77
Urethra PRV $D_{0.1\ cc}$ (Gy)	51.87 ± 0.06	51.08 ± 0.32	−0.80 ± 0.33	< 0.001

beamlet per unit weight.

The clinical target volume (CTV) was defined as the entire prostate gland. The planning target volumes (PTV) were created as PTV1 and PTV2, according to the working group for genitourinary tumors in Japan [28]. PTV1 was defined as the CTV plus 5 mm margins cranially, caudally, and posteriorly, and 10 mm margins laterally and anteriorly. PTV2 was created by adding 2–3 mm margins posteriorly, remaining identical to the CTV cranially and caudally, and matching PTV1 laterally and anteriorly. A 3 mm margin was added to the GTV_{boost} to create the planning boost target, PTV_{boost} (ranging from 1.0 to 6.9 cm^3). These additional margins were established to account for setup uncertainty. Moreover, urethra planning risk volume (PRV) was defined by expanding the urethra with a 1 mm safety margin. Two opposing lateral beams were employed, to deliver the desired RBE-weighted prescription dose of 51.6 Gy in 12 fractions (PTV1 was irradiated for the first eight fractions, and PTV2 for the final four fractions). Prescribed dose was defined as $D_{100\%}$ for PTV2 $\geq$ 95%, which is the current standard CIRT regimen for localized prostate cancer in Japan [28–30]. Furthermore, the maximum dose of the PTV2 should not exceed 105% of the prescribed dose. The target goals and OAR constraints, including RBE-weighted dose metrics and LET_d metrics, are detailed in Table 1.

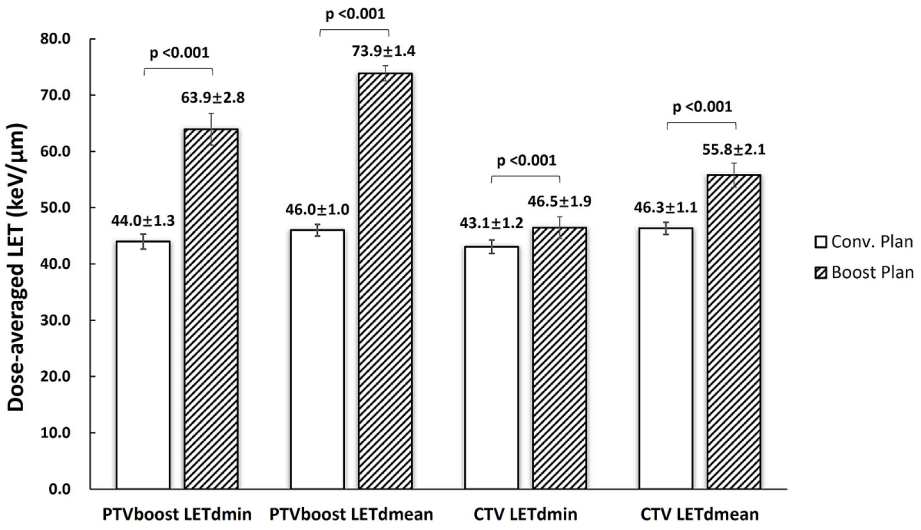

Fig. 3. A grouped bar chart comparing the dose-averaged LET parameters between the conventional plan (white bars) and the boost plan (shadowed bars). The LET_d metrics shown included PTV_{boost} $LET_{d,min}$, PTV_{boost} $LET_{d,mean}$, CTV $LET_{d,min}$, and CTV $LET_{d,mean}$, across all cases. The bars represented the mean values, while the whiskers on the bars indicated the 95% confidence intervals. The mean ± standard deviation was displayed on each bar. The p-value was also provided at the top of each corresponding LET_d metrics group.

PTV_{boost} and urethra PRV were not considered for the conventional plan optimization.

This study designed the conventional plan as usual, and the boost plan was re-optimized for all 12 fractions using the same beam arrangement as the conventional plan. To optimize LET_d within the PTV_{boost}, the maximum LET_d (L_{max}) was set to L + 10 keV/μm, the goal LET_d (L) to L keV/μm, and the minimum LET_d (L_{min}) to L-5 keV/μm [31]. To explore the feasible $LET_{d,min}$ to the PTV_{boost} can be escalated while maintaining the PTV2′s dose coverage and sparing OARs, the L was varied at 50, 60, 70, 75, 80, 90, and 100 keV/μm in the boost plans across all cases. The prescribed RBE-weighted dose of 51.6 Gy was set as 100%. Then, the dose coverage for PTV2 was evaluated to determine the optimal value of L that satisfies the clinical criteria ($D_{max} \leq 105\%$ and $D_{min} \geq 95\%$).

2.3. Planning evaluation and analysis

An analysis of RBE-weighted dose and LET_d distributions was conducted to evaluate the LET painting plans. Dose metrics (including $D_{90\%}$, $D_{50\%}$, D_{max}, and D_{min} of PTV2, as well as dose constraints for the rectum and urethra) along with LET_d metrics ($LET_{d,min}$ and $LET_{d,mean}$ of PTV_{boost} and CTV) in the boost plans were determined and compared to those in the conventional plans. It was deemed acceptable in clinical practice if the mean difference in PTV2′s $D_{90\%}$ and $D_{50\%}$ between the two plans was less than 1% [22]. Furthermore, the dependence of $LET_{d,min}$ on the PTV_{boost} characteristics was analyzed by six anatomical measures, including the size of PTV_{boost} (V_{boost}), the minimum distance between the PTV_{boost} and rectum (d_{rec}) or urethra PRV (d_{ure}), and the height, width, and ratio of height to width of PTV_{boost} in the PTV_{boost} midplane CT slice (h, w, and R_{hw}). If there was an overlap between the PTV_{boost} and the rectum or urethra PRV, the d_{rec} or d_{ure} was defined as the maximum overlapping distance and assigned negative values.

The statistical analysis employed a two-sided t-test with 95% confidence intervals, to compare the conventional and the boost plans (IBM SPSS statistics for Windows, version 28.0). Differences were deemed statistically significant at $p < 0.05$. Additionally, the linear correlation coefficients (R) between the minimum LET_d and the PTV_{boost} geometric features were calculated. A solid linear relationship is indicated if $|R| \geq 0.8$.

3. Results

The PTV2 D_{max} and PTV2 D_{min} of the boost plans when the goal LET_d value (L) varied, are shown in Fig. 1. When the LET_d goal exceeded 75 keV/μm, PTV2 D_{max} exceeded the 105% threshold, and/or PTV2 D_{min} decreased below the 95% threshold. Therefore, the boost plans illustrated in the following were optimized with the objectives of $L_{max} = 85$ keV/μm, $L = 75$ keV/μm, and $L_{min} = 70$ keV/μm in the TPS, respectively.

A comparison of treatment plans for a typical case with a PTV_{boost} adjacent to both the rectum and urethra PRV, including RBE-weighted dose and LET_d distributions for the conventional and boost plans, as well as their corresponding dose-volume histogram (DVH) and LET_d-volume histogram (LVH), was presented in Fig. 2. The DVHs of targets and OARs in the boost plan were nearly identical to those in the conventional plan. For this case, PTV2′s $D_{90\%}$, $D_{50\%}$, D_{max}, and D_{min} in the conventional plan were 99.2%, 99.9%, 101.3%, and 98.7%, respectively. Corresponding doses in the boost plan were 98.4%, 99.9%, 101.7% and 95.9%. Without obvious differences in PTV2′s dose coverage between the two treatment plans, the boost plan effectively redistributed high LET_d to the specific PTV_{boost} region, resulting in markedly higher LET_d deposition in the PTV_{boost} compared to the conventional plan, as shown in Fig. 2d and 2f.

For the 15 cases, the mean difference in PTV2′s $D_{90\%}$ and $D_{50\%}$ between the conventional and the boost plans were −0.9 ± 0.1% and −0.1 ± 0.1%, respectively, showing that the LET painting delivered clinically comparable RBE-weighted dose coverage to the target (the mean difference was less than 1%). Table 2 lists the RBE-weighted dose metrics results for OAR constraints across all cases. No statistically significant differences were observed for the rectum ($p > 0.05$). Moreover, the boost plan significantly reduced the $D_{0.1\ cc}$ of the urethra PRV ($p < 0.001$) when both LET_d optimization and urethra PRV constraints were considered simultaneously.

The comparisons of $LET_{d,min}$ and $LET_{d,mean}$ within the PTV_{boost} for all cases between the two plans were 44.0 ± 1.3 keV/μm vs. 63.9 ± 2.8 keV/μm ($p < 0.001$) and 46.0 ± 1.0 keV/μm vs. 73.9 ± 1.4 keV/μm ($p < 0.001$), respectively. Similar results were observed for the CTV, as illustrated in Fig. 3. It was evident that LET painting delivered higher LET_d values throughout the PTV_{boost} and CTV, while in the conventional plans, high LET_d values were not delivered within the high-risk targets but to the periphery of the PTV2, as shown in Fig. 2c.

The linear correlation analysis between the minimum LET_d and

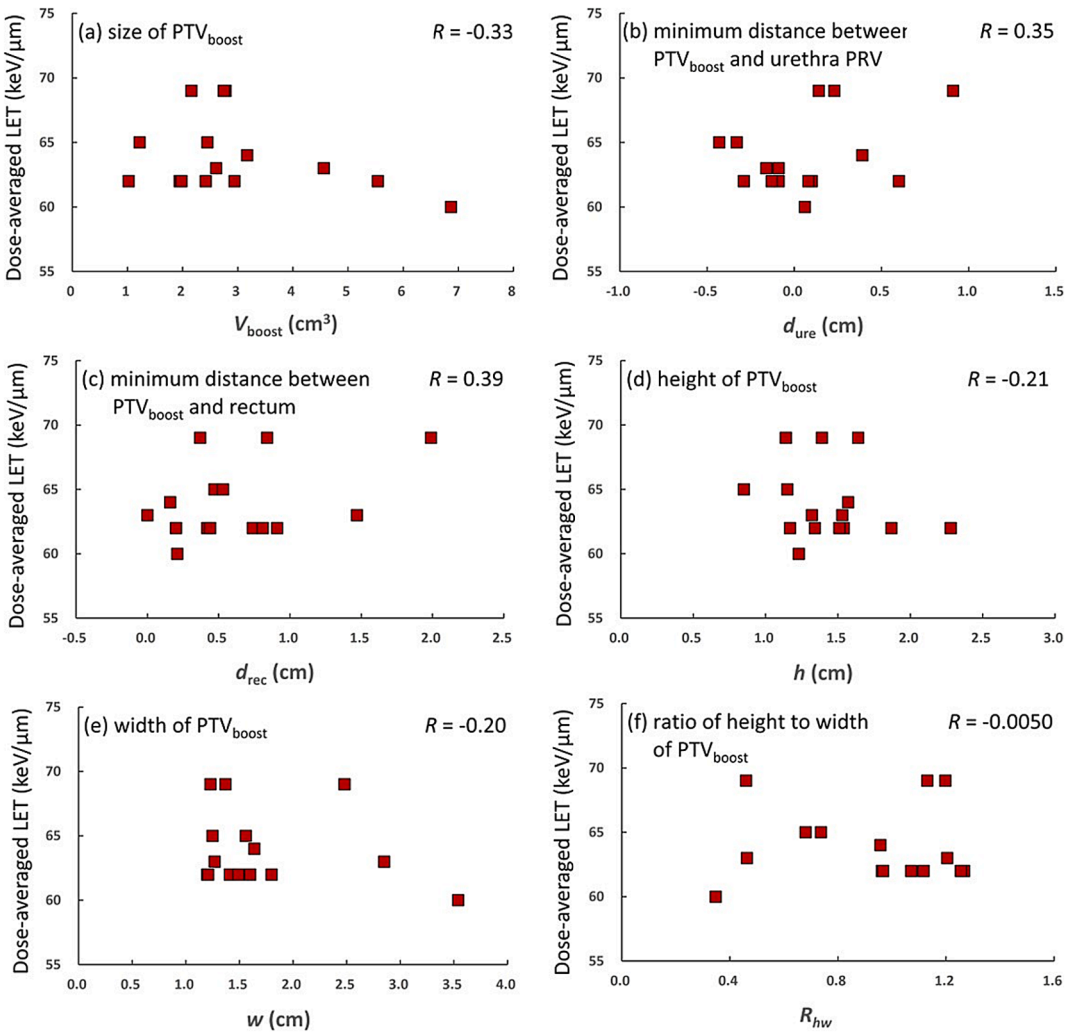

Fig. 4. The scatter plots and linear correlation analysis between the minimum LET_d and geometric parameters of PTV_{boost} for 15 cases' boost plans were presented. These parameters included (a) The size of PTV_{boost}, V_{boost}, (b)The minimum distance between PTV_{boost} and the urethra PRV, d_{ure}, (c) The minimum distance between PTV_{boost} and the rectum, d_{rec}, (d) The height of PTV_{boost} in the PTV_{boost} midplane slice, h, (e) The width of PTV_{boost} in the PTV_{boost} midplane slice, w, and (f) The ratio of height to width of PTV_{boost} in the PTV_{boost} midplane slice, R_{hw}. The linear correlation coefficient (R-value) was displayed in the top right corner of each scatter plot.

geometric parameters of PTV_{boost} for 15 cases' boost plans was presented in Fig. 4. Since the correlation coefficients were relatively low ($R = -0.33$ for V_{boost}, $R = 0.35$ for d_{ure}, $R = 0.39$ for d_{rec}, $R = -0.21$ for h, $R = -0.20$ for w, and $R = -0.01$ for R_{hw}), there was no strong linear relationship between $LET_{d,min}$ and any of the six geometric factors.

4. Discussion

The proposed focal LET_d boost demonstrated clinical feasibility for prostate carbon-ion radiotherapy. Compared to the conventional plans, the boost plans delivered clinically acceptable dose coverage and OAR sparing, with significant increases in minimum and mean LET_d for PTV_{boost} and CTV. Additionally, the boost plans can effectively deliver high LET_d values without being influenced by the geometric variability of the PTV_{boost}.

The published in vitro study [19] and retrospective clinical studies [20,21] indicated that the minimum LET_d was associated with tumor control probability, with threshold LET_d values for recurrence being 40 keV/μm for chondrosarcomas and 44 keV/μm for pancreatic cancer. The notable finding was that the minimum LET_d values in conventional treatment plans for prostate cancer patients in our hospital were sufficiently high compared to established thresholds. However, significant variations among patients—such as pathological stage, cancer cell type, and hypoxia status—mean that these statistical thresholds cannot definitively predict non-recurrence for individuals. Consequently, employing boost plans that deliver higher LET_d to the DIL volume may enhance local control for high-risk prostate cancer patients. Furthermore, unlike photon and proton therapies, where the feasibility of dose-escalation was sensitive to the proximity of OARs [9,12–15], the effectiveness in increasing LET_d is not affected by inter-patient anatomical variability. This approach facilitated clinical translation and simplified treatment planning for focal boost strategies.

Admittedly, some challenges remain to be addressed. This study was only an *in-silico* treatment planning exploration, and the clinical efficacy and safety of the focal LET_d boost required further validation through rigorous clinical trials. One key limitation is that we did not consider LET_d constraints for OARs during the LET optimization. While it is reasonable to assume that LET painting with a comparable RBE-weighted dose would not worsen NTCP—given that the OER of normal tissues would remain unchanged in their non-hypoxic state—this assumption needs careful validation. Supporting this assumption, a retrospective study found no correlation between LET_d and ≥ grade 3 late rectal side effects in carbon-ion radiotherapy [32]. Similarly, Mori et al. reported that LET_d parameters were not associated with sacral insufficiency fracture [33]. However, it is important to note that Nachankar et al. emphasized that RBE-weighted dose-filtered LET_d

could influence side effects on the sacral nerves [34]. This contradiction indicates that while our hypothesis holds in some contexts, it may not be universally applicable. Given these complexities, follow-up observations are necessary. Therefore, further clinical trials should consider various RBE-weighted dose and LET_d-related parameters to comprehensively evaluate the potential impacts of delivering a focal LET_d boost in CIRT.

Another limitation was the lack of robust optimization during LET painting. However, the setup uncertainty could be addressed by adding margins to the CTV-PTV and GTV_{boost}-PTV_{boost}. Also, the range uncertainty was accounted for using an optimization parameter called "smearing," set to 2 mm for the proximal region and 3 mm for the distal region during treatment planning. Moreover, in this study, the boost region was treated as a small tumor (the maximum volume of PTV_{boost} was 6.9 cm^3), and its robustness was unlikely to deteriorate due to the high LET_d transferred to the target [35].

In conclusion, this study demonstrated that significantly increased LET_d values can be achieved within the PTV_{boost} compared to conventional approaches, while maintaining target coverage and satisfying rectum and urethra constraints. Furthermore, this was demonstrated for a range of different boost volumes and shapes, highlighting its potential for clinical application in prostate cancer carbon-ion radiotherapy and paving the way for future clinical trials.

CRediT authorship contribution statement

Bo Zhao: Writing – original draft, Conceptualization, Methodology, Data curation, Investigation. **Nobuyuki Kanematsu:** Writing – review & editing, Conceptualization, Methodology, Project administration. **Shuri Aoki:** Writing – review & editing, Methodology, Investigation, Resources. **Shinichiro Mori:** Writing – review & editing, Conceptualization, Methodology. **Hideyuki Mizuno:** Writing – review & editing, Data curation. **Takamitsu Masuda:** Writing – review & editing, Investigation, Software. **Hideyuki Takei:** Writing – review & editing, Investigation. **Hitoshi Ishikawa:** Writing – review & editing, Supervision, Conceptualization, Funding acquisition.

Funding

This work was supported by JSPS KAKENHI Grant Number JP21K07715.

Declaration of competing interest

The authors declare that they have no known competing financial interests or personal relationships that could have appeared to influence the work reported in this paper.

Acknowledgments

We acknowledge Dr. Toshiyuki Shirai, Dr. Taku Inaniwa, and Dr. Yusuke Nomura for their discussions and suggestions. We thank Dr. Wataru Furuichi, Dr. Katsumi Aoki, and Dr. Taku Nakaji for the additional workload during this investigation.

References

[1] Zaorsky NG, Palmer JD, Hurwitz MD, Keith SW, Dicker AP, Den RB. What is the ideal radiotherapy dose to treat prostate cancer? A meta-analysis of biologically equivalent dose escalation. Radiother Oncol 2015;115:295–300. https://doi.org/10.1016/j.radonc.2015.05.011.

[2] McKeown SR. Defining normoxia, physoxia and hypoxia in tumours-implications for treatment response. Br J Radiol 2014;87:20130676. https://doi.org/10.1259/bjr.20130676.

[3] Chen ME, Johnston DA, Tang K, Babaian RJ, Troncoso P. Detailed mapping of prostate carcinoma foci: biopsy strategy implications. Cancer 2000;89:1800–9. https://doi.org/10.1002/1097-0142(20001015)89:8<1800::aid-cncr21>3.0.co;2-d.

[4] Guimond E, Lavallée M-C, Foster W, Éric V, Guay K, Martin AG. Impact of a dominant intraprostatic lesion (DIL) boost defined by sextant biopsy in permanent I-125 prostate implants on biochemical disease free survival (bDFS) and toxicity outcomes. Radiother Oncol 2019;133:62–7. https://doi.org/10.1016/j.radonc.2018.12.027.

[5] Aizawa R, Otani T, Ogata T, Moribata Y, Kido A, Akamatsu S, et al. Spatial pattern of intraprostatic recurrence after definitive external-beam radiation therapy for prostate cancer: implications for focal boost to intraprostatic dominant lesion. Adv Radiat Oncol 2024;9:101489. https://doi.org/10.1016/j.adro.2024.101489.

[6] Gomez-Iturriaga A, Casquero F, Urresola A, Ezquerro A, Lopez JI, Espinosa JM, et al. Dose escalation to dominant intraprostatic lesions with MRI-transrectal ultrasound fusion High-Dose-Rate prostate brachytherapy. Prospective phase II trial. Radiother Oncol 2016;119:91–6. https://doi.org/10.1016/j.radonc.2016.02.004.

[7] Zhao Y, Haworth A, Rowshanfarzad P, Ebert MA. Focal boost in prostate cancer radiotherapy: a review of planning studies and clinical trials. Cancers 2023;15:4888. https://doi.org/10.3390/cancers15194888.

[8] Kerkmeijer LGW, Groen VH, Pos FJ, Haustermans K, Monninkhof EM, Smeenk RJ, et al. Focal boost to the intraprostatic tumor in external beam radiotherapy for patients with localized prostate cancer: results from the FLAME randomized Phase III Trial. J Clin Oncol 2021;39:787–96. https://doi.org/10.1200/JCO.20.02873.

[9] Groen VH, van Schie M, Zuithoff NPA, Monninkhof EM, Kunze-Busch M, de Boer JCJ, et al. Urethral and bladder dose-effect relations for late genitourinary toxicity following external beam radiotherapy for prostate cancer in the FLAME trial. Radiother Oncol 2022;167:127–32. https://doi.org/10.1016/j.radonc.2021.12.027.

[10] Morris WJ, Tyldesley S, Rodda S, Halperin R, Pai H, McKenzie M, et al. Androgen suppression combined with elective nodal and dose escalated radiation therapy (the ASCENDE-RT Trial): an analysis of survival endpoints for a randomized trial comparing a low-dose-rate brachytherapy boost to a dose-escalated external beam boost for high- and intermediate-risk prostate cancer. Int J Radiat Oncol Biol Phys 2017;98:275–85. https://doi.org/10.1016/j.ijrobp.2016.11.026.

[11] Incrocci L, Wortel RC, Alemayehu WG, Aluwini S, Schimmel E, Krol S, et al. Hypofractionated versus conventionally fractionated radiotherapy for patients with localised prostate cancer (HYPRO): final efficacy results from a randomised, multicentre, open-label, phase 3 trial. Lancet Oncol 2016;17:1061–9. https://doi.org/10.1016/S1470-2045(16)30070-5.

[12] Blake SW, Stapleton A, Brown A, Curtis S, Ash-Miles J, Dennis E, et al. A study of the clinical, treatment planning and dosimetric feasibility of dose painting in external beam radiotherapy of prostate cancer. Phys Imaging Radiat Oncol 2020;15:66–71. https://doi.org/10.1016/j.phro.2020.07.005.

[13] Murray LJ, Lilley J, Thompson CM, Cosgrove V, Mason J, Sykes J, et al. Prostate stereotactic ablative radiation therapy using volumetric modulated arc therapy to dominant intraprostatic lesions. Int J Radiat Oncol Biol Phys 2014;89:406–15. https://doi.org/10.1016/j.ijrobp.2014.01.042.

[14] Dankulchai P, Alonzi R, Lowe GJ, Burnley J, Padhani AR, Hoskin PJ. Optimal source distribution for focal boosts using high dose rate (HDR) brachytherapy alone in prostate cancer. Radiother Oncol 2014;113:121–5. https://doi.org/10.1016/j.radonc.2014.09.001.

[15] Wang T, Zhou J, Tian S, Wang Y, Patel P, Jani AB, et al. A planning study of focal dose escalations to multiparametric MRI-defined dominant intraprostatic lesions in prostate proton radiation therapy. Br J Radiol 2020;93:20190845. https://doi.org/10.1259/bjr.20190845.

[16] Hu W, Li P, Hong Z, Guo X, Pei Y, Zhang Z, et al. Functional imaging-guided carbon ion irradiation with simultaneous integrated boost for localized prostate cancer: study protocol for a phase II randomized controlled clinical trial. Trials 2022;23:934. https://doi.org/10.1186/s13063-022-06798-5.

[17] Masuda T, Inaniwa T. Effects of cellular radioresponse on therapeutic helium-, carbon-, oxygen-, and neon-ion beams: a simulation study. Phys Med Biol 2024;69. https://doi.org/10.1088/1361-6560/ad1f87.

[18] Sokol O, Krämer M, Hild S, Durante M, Scifoni E. Kill painting of hypoxic tumors with multiple ion beams. Phys Med Biol 2019;64:045008. https://doi.org/10.1088/1361-6560/aafe40.

[19] Tinganelli W, Durante M, Hirayama R, Krämer M, Maier A, Kraft-Weyrather W, et al. Kill-painting of hypoxic tumours in charged particle therapy. Sci Rep 2015;5:17016. https://doi.org/10.1038/srep17016.

[20] Hagiwara Y, Bhattacharyya T, Matsufuji N, Isozaki Y, Takiyama H, Nemoto K, et al. Influence of dose-averaged linear energy transfer on tumour control after carbon-ion radiation therapy for pancreatic cancer. Clin Transl Radiat Oncol 2019;21:19–24. https://doi.org/10.1016/j.ctro.2019.11.002.

[21] Matsumoto S, Lee SH, Imai R, Inaniwa T, Matsufuji N, Fukahori M, et al. Unresectable chondrosarcomas treated with carbon ion radiotherapy: relationship between dose-averaged linear energy transfer and local recurrence. Anticancer Res 2020;40:6429–35. https://doi.org/10.21873/anticanres.14664.

[22] Koto M, Ikawa H, Inaniwa T, Imai R, Shinoto M, Takiyama H, et al. Dose-averaged LET optimized carbon-ion radiotherapy for head and neck cancers. Radiother Oncol 2024;194:110180. https://doi.org/10.1016/j.radonc.2024.110180.

[23] Draulans C, van der Heide UA, Haustermans K, Pos FJ, van der Voort van Zyp J, De Boer H, et al. Primary endpoint analysis of the multicentre phase II hypo-FLAME trial for intermediate and high risk prostate cancer. Radiother Oncol 2020;147:92–8. https://doi.org/10.1016/j.radonc.2020.03.015.

[24] van Schie MA, Dinh CV, Houdt PJV, Pos FJ, Heijmink SWTJP, Kerkmeijer LGW, et al. Contouring of prostate tumors on multiparametric MRI: Evaluation of clinical delineations in a multicenter radiotherapy trial. Radiother Oncol 2018;128:321–6. https://doi.org/10.1016/j.radonc.2018.04.015.

[25] Inaniwa T, Kanematsu N, Matsufuji N, Kanai T, Shirai T, Noda K, et al. Reformulation of a clinical-dose system for carbon-ion radiotherapy treatment

planning at the National Institute of Radiological Sciences. Japan Phys Med Biol 2015;60:3271–86. https://doi.org/10.1088/0031-9155/60/8/3271.
[26] Inaniwa T, Furukawa T, Kase Y, Matsufuji N, Toshito T, Matsumoto Y, et al. Treatment planning for a scanned carbon beam with a modified microdosimetric kinetic model. Phys Med Biol 2010;55:6721–37. https://doi.org/10.1088/0031-9155/55/22/008.
[27] Inaniwa T, Kanematsu N, Noda K, Kamada T. Treatment planning of intensity modulated composite particle therapy with dose and linear energy transfer optimization. Phys Med Biol 2017;62:5180–97. https://doi.org/10.1088/1361-6560/aa68d7.
[28] Sato H, Kasuya G, Ishikawa H, Nomoto A, Ono T, Nakajima M, et al. Long-term clinical outcomes after 12-fractionated carbon-ion radiotherapy for localized prostate cancer. Cancer Sci 2021;112:3598–606. https://doi.org/10.1111/cas.15019.
[29] Mori S, Takei Y, Shirai T, Hara Y, Furukawa T, Inaniwa T, et al. Scanned carbon-ion beam therapy throughput over the first 7 years at National Institute of Radiological Sciences. Phys Med 2018;52:18–26. https://doi.org/10.1016/j.ejmp.2018.06.002.
[30] Ishikawa H, Tsuji H, Murayama S, Sugimoto M, Shinohara N, Maruyama S, et al. Particle therapy for prostate cancer: The past, present and future. Int J Urol 2019;26:971–9. https://doi.org/10.1111/iju.14041.
[31] Kohno R, Koto M, Ikawa H, Lee SH, Sato K, Hashimoto M, et al. High-linear energy transfer irradiation in clinical carbon-ion beam with the linear energy transfer painting technique for patients with head and neck cancer. Adv Radiat Oncol 2023;9:101317. https://doi.org/10.1016/j.adro.2023.101317.
[32] Okonogi N, Matsumoto S, Fukahori M, Furuichi W, Inaniwa T, Matsufuji N, et al. Dose-averaged linear energy transfer per se does not correlate with late rectal complications in carbon-ion radiotherapy. Radiother Oncol 2020;153:272–8. https://doi.org/10.1016/j.radonc.2020.08.029.
[33] Mori Y, Okonogi N, Matsumoto S, Furuichi W, Fukahori M, Miyasaka Y, et al. Effects of dose and dose-averaged linear energy transfer on pelvic insufficiency fractures after carbon-ion radiotherapy for uterine carcinoma. Radiother Oncol 2022;177:33–9. https://doi.org/10.1016/j.radonc.2022.10.008.
[34] Nachankar A, Schafasand M, Hug E, Martino G, Góra J, Carlino A, et al. Sacral-nerve-sparing planning strategy in pelvic sarcomas/chordomas treated with carbon-ion radiotherapy. Cancers (Basel) 2024;16:1284. https://doi.org/10.3390/cancers16071284.
[35] Fredriksson A, Glimelius L, Bokrantz R. The LET trilemma: Conflicts between robust target coverage, uniform dose, and dose-averaged LET in carbon therapy. Med Phys 2023;50:7338–48. https://doi.org/10.1002/mp.16771.